Pankaj Agarwal,[1] *Mark E. Orazem,*[1] *and Luis H. Garcia-Rubio*[2]

Application of the Kramers-Kronig Relations in Electrochemical Impedance Spectroscopy

REFERENCE: Agarwal, P., Orazem, M. E., and Garcia-Rubio, L. H., "Application of the Kramers-Kronig Relations in Electrochemical Impedance Spectroscopy," *Electrochemical Impedance: Analysis and Interpretation, ASTM STP 1188,* J. R. Scully, D. C. Silverman, and M. W. Kendig, Eds., American Society for Testing and Materials, Philadelphia, 1993, pp. 115–139.

ABSTRACT: The Kramers-Kronig equations and the current methods used to apply them to electrochemical impedance spectra are reviewed. Measurement models are introduced as a tool for identification of the frequency-dependent error structure of impedance data and for evaluating the consistency of the data with the Kramers-Kronig relations. Through the use of a measurement model, experimental data can be checked for consistency with the Kramers-Kronig relations without explicit integration of the Kramers-Kronig relations; therefore, inaccuracies associated with extrapolation of an incomplete frequency spectrum are resolved. The measurement model can be used to determine whether the residual errors in the regression are due to an inadequate model, failure of data to conform to the Kramers-Kronig assumptions, or noise.

KEYWORDS: Kramers-Kronig relations, impedance spectroscopy, error structure, measurement models, deconvolution

In principle, the Kramers-Kronig relations can be used to determine whether the impedance spectrum of a given system has been influenced by time-dependent phenomena. Although this information is critical to the analysis of impedance data, the Kramers-Kronig relations have not found widespread use in the analysis and interpretation of electrochemical impedance spectroscopy data due to difficulties with their application. The integral relations require data for frequencies ranging from zero to infinity, but the experimental frequency range is often constrained by instrumental limitations or by noise attributable to the instability of the electrode.

The Kramers-Kronig relations have been applied to electrochemical systems by direct integration of the equations, experimental observation of stability and linearity, or regression of electrical circuit models to the data. Each of these approaches has its advantages and disadvantages. This paper will review the Kramers-Kronig equations and the methods used to apply them to electrochemical impedance spectra. This paper will then suggest that the disadvantages associated with current methods used to check experimental data for consistency with the Kramers-Kronig relations can be circumvented by application of measurement models to impedance spectra.

[1]Graduate student and professor, respectively, Department of Chemical Engineering, University of Florida, Gainesville, FL 32611.
[2]Professor, Department of Chemical Engineering, University of South Florida, Tampa, FL 33620.

The Kramers-Kronig Relations

The Kramers-Kronig relations, developed for the field of optics, are integral equations which constrain the real and imaginary components of complex quantities for systems that satisfy conditions of causality, linearity, and stability [*1–4*]. Bode [*5*] extended the concept to electrical impedance and tabulated various forms of the Kramers-Kronig relations. Several transformations used in the electrochemical literature are shown. The imaginary part of the impedance can be obtained from the real part of the impedance spectrum through

$$Z_i(\omega) = -\left(\frac{2\omega}{\pi}\right)\int_0^\infty \frac{Z_r(x) - Z_r(\omega)}{x^2 - w^2}\,dx, \tag{1}$$

where $Z_r(\omega)$ and $Z_i(\omega)$ are the real and imaginary components of the impedance as functions of frequency ω. The real part of the impedance spectrum can be obtained from the imaginary part through

$$Z_r(\omega) = Z_r(\infty) + \frac{2}{\pi}\int_0^\infty \frac{x\,Z_i(x) - \omega Z_i(\omega)}{x^2 - w^2}\,dx, \tag{2}$$

if the high-frequency asymptote for the real part of the impedance is known, and through

$$Z_r(\omega) = Z_r(0) + \frac{2\omega}{\pi}\int_0^\infty \frac{x/\omega Z_i(x) - Z_i(\omega)}{x^2 - w^2}\,dx \tag{3}$$

if the zero-frequency asymptote for the real part of the impedance is known. A relationship between the phase angle $\phi(\omega)$ and modulus $|Z(\omega)|$ is also available, e.g.,

$$\phi(\omega) = \frac{2\omega}{\pi}\int_0^\infty \frac{\ln\,(|Z(x)|}{x^2 - w^2}\,dx \tag{4}$$

In response to the integration limits, a fourth constraint, which the impedance approaches finite values at frequency limits of zero and infinity, is commonly added. This constraint, sometimes claimed to prevent application of the Kramers-Kronig relations to capacitive systems, is in fact not needed because a simple variable substitution [*5*] can be used if the imaginary part of the impedance tends to infinity according to $1/\omega$ as $\omega \rightarrow \omega_0$ (see also Ref *6*).

Review of Methods for Determining Consistency with the Kramers-Kronig Relations

The usual approach in interpreting impedance spectra is to regress a model to the data. The models employed are typically linear and assume conditions of a sinusoidal steady state. It is important, therefore, that the impedance response be characteristic of a system that is causal, linear, and stable. The condition of linearity can be achieved by using sufficiently small amplitude perturbations. The condition of stability requires that the sys-

tem return to its original condition when the perturbing signal is terminated. An additional implied constraint of stationary behavior may be difficult to achieve in electrochemical systems (such as corrosion) where the electrode may change significantly during the time required to collect impedance data. It is therefore of practical importance to the experimentalist to know whether the data taken do in fact satisfy the Kramers-Kronig relations. The approaches taken to ascertain the degree of consistency include direct integration of the Kramers-Kronig relations, experimental replication of data, and regression of electrical circuit analogues to the data.

Direct Integration of Kramers-Kronig Relations

The Kramers-Kronig relations provide a unique transformation that can be used to predict one component of the impedance if the other is known over the frequency limits of zero to infinity. The usual way of using the Kramers-Kronig equations, therefore, is to calculate the imaginary component of impedance from the measured real component using, for example, Eq 1, and to compare the values obtained to the experimental imaginary component. Alternatively, the real component of impedance can be calculated from the measured imaginary values using Eqs 2 or 3. The major difficulty in applying this approach is that the measured frequency range may not be sufficient to allow integration over the frequency limits of zero to infinity. Therefore, discrepancies between experimental data and the impedance component predicted through application of the Kramers-Kronig relations could be attributed to use of a frequency domain that is too narrow as well as to failure to satisfy the constraints of the Kramers-Kronig equations. The Kramers-Kronig relations can, in principle, be applied with a suitable extrapolation of the data into the unmeasured frequency domain. Several methods for extrapolation have appeared in the electrochemical literature.

Kendig and Mansfeld [7] proposed extrapolating an impedance spectrum into the low-frequency domain under the assumption that the imaginary impedance is symmetric, thus, the polarization resistance R_p, otherwise obtained from

$$R_p = Z_r(\infty) - Z_r(0) = \frac{2}{\pi}\int_0^{\infty}\left[\frac{Z_i(x)}{x}\right]dx \tag{5}$$

would be obtained from

$$R_p = Z_r(\infty) - Z_r(0) = \frac{4}{\pi}\int_{\omega_{max}}^{\infty}\left[\frac{Z_i(x)}{x}\right]dx \tag{6}$$

where ω_{max} is the frequency at which the maximum in the imaginary impedance is observed. This approach is limited to systems which can be modeled by a single relaxation time constant [8,9]. The limitation to a single time constant is severe because multiple elementary processes with different characteristic time constants are usually observed in electrochemical impedance spectra.

Macdonald and Urquidi-Macdonald [8] have presented an approach based on extrapolating polynomials fit to the data. The experimental frequency domain was divided into several segments, and the individual impedance components $Z_r(\omega)$ and $Z_i(\omega)$ were fitted to a polynomial expression given by

$$Z_r = \sum_{k=0}^{n} a_k \omega^k \tag{7}$$

and

$$Z_i = \sum_{k=0}^{n} a_k \omega^k \tag{8}$$

which was extrapolated into the unmeasured frequency domain. The Kramers-Kronig equation (e.g., Eq 1 or 3) was integrated numerically using the extrapolated piece-wise polynomial fit for either the real or the imaginary component of the impedance, respectively [*10,11,12*]. While the extrapolation algorithm was applied successfully to a variety of systems (including synthetic impedance data derived from equivalent electrical circuits and experimental systems such as TiO_2-coated carbon steel in aqueous HCl/KCl solutions), such extrapolation of polynomials is unreliable over a broad frequency range.

Haili [*13*] provided an alternative approach based on the expected asymptotic behavior of a typical electrochemical system. For extrapolation to $\omega = 0$, the imaginary component $Z_i(\omega)$ was assumed to be proportional to ω as $\omega \rightarrow 0$ consistent with the behavior of a Randles-type equivalent circuit. This approach would apply as well to a Warburg impedance, which is also nearly proportional to ω as $\omega \rightarrow 0$. The real impedance approaches a constant limit which is the sum of the Ohmic solution resistance and the polarization resistance. The extrapolation in this region involves only one adjustable parameter whose value will approach $Z_r(\omega_{min})$ if ω_{min} is sufficiently small. At high frequencies, the imaginary component was assumed to be inversely proportional to frequency as $\omega \rightarrow \infty$ and the real component was assumed to approach a constant equivalent to the Ohmic solution resistance R_∞. The method of Haili guarantees well-behaved extrapolation of the impedance spectrum at upper and lower frequency limits with only five adjustable parameters. Haili's work confirmed the importance of extrapolating impedance data to both zero and infinite frequency when evaluating the Kramers-Kronig relations.

Esteban and Orazem, et al. [*14,15*] presented an approach which circumvented the problems associated with extrapolations of polynomials and yet avoided making *a priori* assumption of a model for asymptotic behavior. Esteban and Orazem suggested that, instead of predicting the imaginary impedance from the measured real impedance using Eq 1 or, alternatively, predicting the real impedance from the measured imaginary values using Eq 2 or 3, both equations could be used simultaneously to calculate the impedance below the lowest measured frequency ω_{min}. The low-frequency limit ω_0 is an adjustable parameter that is typically three or four orders of magnitude smaller than ω_{min}. The calculated impedance, in the domain $\omega_0 \leq \omega < \omega_{min}$, "forces" the experimental data set to satisfy the Kramers-Kronig relations in the frequency domain $\omega_0 \leq \omega \leq \omega_{max}$. The parameter ω_0 is chosen to satisfy the requirements that the real component of the impedance spectrum attains an asymptotic value and that the imaginary component approaches zero as $\omega \rightarrow \omega_0$. Internal consistency between the impedance components also requires that the calculated functions be continuous with the experimental data at ω_{min}. These requirements cannot simultaneously be satisfied by data from systems that do not satisfy the constraints of the Kramers-Kronig relations; therefore, discontinuities between experimental and extrapolated values were attributed to inconsistency with the Kramers-Kronig relations. The approach described by Esteban and Orazem [*14,15*] is different from other algorithms presented here because the Kramers-Kronig relations themselves were used to extrapolate

data to frequencies below the lowest measured frequency. Extrapolation of polynomials or *a priori* assumption of a model was thereby avoided.

While each of the algorithms described here have been applied to some experimental data with success, any approach toward extrapolation can be applied over only a small frequency range and cannot be applied at all if the experimental frequency range is so small that the data do not show a maximum in the imaginary impedance. The extrapolation approach for evaluating consistency with the Kramers-Kronig relations cannot be applied, therefore, to a broad class of experimental systems for which the unmeasured portion of the impedance spectrum at low frequencies is not merely part of a "tail" but instead represents a significant portion of the impedance spectrum.

Experimental Checks for Consistency

Experimental methods can be applied to check whether impedance data conform to the Kramers-Kronig assumptions. A check for linear response can be made by observing whether spectra obtained with different magnitudes of the forcing function are replicate. Stationary behavior can be identified experimentally by replication of the impedance spectrum. Spectra are replicate if the spectra agree within the expected frequency-dependent measurement error. If the experimental frequency range is sufficient, the extrapolation of the impedance spectrum to zero frequency can be compared to the corresponding values obtained from separate steady state experiments.

The experimental approach to evaluating consistency with the Kramers-Kronig relations shares constraints with direct integration of the Kramers-Kronig equations. Because extrapolation is required, the comparison of the dc limit of impedance spectra to steady state measurement is possible only for systems for which a reasonably complete spectrum can be obtained. Experimental approaches for verifying consistency with the Kramers-Kronig relations by replication are further limited in that, without an *a priori* estimate for the confidence limits of the experimental data, the comparison is more qualitative than quantitative. A method is therefore needed to evaluate the error structure, or frequency-dependent confidence interval, for the data that would be obtained in the absence of nonstationary behavior.

Regression of Electrical Circuit Analogues

Electrical circuits consisting of passive and distributed elements satisfy the Kramers-Kronig relations (see, for example, the discussion in Refs *16*, *17*, and *18*). Therefore, successful regression of an electrical circuit analogue to experimental data implies that the data satisfy the Kramers-Kronig relations [*19,20*]. This approach has the obvious advantage that integration over an infinite frequency domain is not required; therefore, a portion of an incomplete spectrum can be identified as being consistent without use of extrapolation algorithms.

It should be noted that the regression is, however, sensitive to the weighting applied to the data, an important consideration for impedance data which vary over many orders of magnitude [*21*]. With no weighting (or unity weighting), the real part of the spectrum at low frequencies and the imaginary part of the spectrum at intermediate frequencies are emphasized. Information about physical processes that influence the spectrum at high frequencies may therefore be lost. A better approach is to provide proportional weighting to each data point, achieved by dividing the objective function at each frequency by the experimental observation at that frequency. The processes that appear at high-frequency are given the same weight in the regression as the processes that are important at low-

frequency. The proportional weighting approach has the disadvantage that the regression can be overly influenced by the portions of the spectrum that have the largest uncertainty. The most desirable approach, therefore, is to divide the objective function at each frequency by the variance of the experimental observation at that frequency [21]. Normalization by the variance will yield proportional weighting if the percent error is not a function of frequency. The problem here is that consistency is determined by regression of a model, and the most reliable regression is obtained only if the frequency dependence of the error structure of the data is known. Also, *a priori* knowledge of the error structure may be needed to decide whether a given regression provides a "good fit." As an alternative to *a priori* knowledge of the error structure, Macdonald has recently suggested that model parameters for error structure be included in the regression of a model to data [22,23].

Perhaps the major problem with the use of electrical circuit models to determine consistency is that interpretation of a "poor fit" is ambiguous. A poor fit is not necessarily the result of an inconsistency of the data with the Kramers-Kronig relations. A poor fit could also be attributed to use of an inadequate model or to regression to a local rather than global minimum (caused perhaps by a poor initial guess).

Application of Measurement Models

In this work, models are classified as being one of two types: process models or measurement models. Process models are used to predict the response of a system from physical phenomena that are hypothesized to be important. Regression of process models to data allows identification of physical parameters based upon the original hypothesis. In contrast, measurement models are built by sequential regression of line shapes to the data. This type model can be used to identify characteristics of the data set that could facilitate selection of an appropriate process model.

The regression of measurement models as a means of determining consistency with the Kramers-Kronig relations is an extension to the use of electrical circuit analogues. Because the model itself is consistent with the Kramers-Kronig relations, successful regression of the model to a given spectrum implies that the data are consistent. Integration over zero to infinity in frequency is not required. The measurement model is composed of a summation of lineshapes that will, with a sufficient number of terms, provide a statistically adequate fit to any consistent data set. Use of the measurement model eliminates the ambiguity in the interpretation of a "poor fit" to the data. Since the model will provide an adequate representation of a consistent spectrum, failure to fit the data can be attributed to inconsistency with the Kramers-Kronig relations. Another result of the adequacy of the model is that the model can be used to identify the frequency-dependent error structure of impedance spectra. The error structure can then be used to weight the data during regression and to provide a means of deciding whether a given regression provided a "good fit." In this section, the measurement model is presented along with a demonstration of applicability to impedance data, its use in determining the frequency-dependent error structure, and its use to determine consistency with the Kramers-Kronig relations.

Structure of Measurement Model

A simple measurement model was obtained for electrochemical impedance spectroscopy [24] by analogy to the classical theories of optical dispersion in which the complex dielectric constant is calculated as a function of the frequency of light [25,26,27]. Since the line shape of the Debye model for the complex dielectric constant was similar to that seen for the complex impedance, an analogue of the multiple Debye model was used, i.e.,

$$Z(\omega) = Z_0 + \sum_k \frac{\Delta_k}{(1 + j\tau_k\omega)} \tag{9}$$

which corresponds to the Voight model (Fig. 1) in series with a solution resistance. The time constant τ_k for element k is equivalent to R_kC_k in the Voight model, and Δ_k is equivalent to R_k. The impedance response of a single Voight element is usually attributed to the electrical response of a linearized electrochemical reaction [*28,29*]. Equation 9 satisfies one requirement of a measurement model in that it is consistent with the Kramers-Kronig relations.

The tenets underlying the use of measurement models for impedance spectroscopy are:

(1) By including a sufficient number of terms, a general measurement model based on Eq 9 can fit impedance data for typical stationary electrochemical systems.
(2) Because the measurement model does fit stationary impedance data, an inability to fit an impedance spectrum can be attributed to failure of the data to conform to the assumptions of the Kramers-Kronig relations rather than to failure of the model. Thus, the measurement model can be used to assess the consistency of impedance data with the Kramers-Kronig relations without integration.

Demonstration of Applicability to Impedance Spectra

The measurement model presented here is most effective in modeling systems that can be modeled otherwise with passive elements such as resistors, capacitors, and inductors. It is perhaps no surprise that, with only two elements, the measurement model can provide a good representation of a circuit developed for painted metals that does not include diffusion or constant phase elements [*30*]. The electrical circuit is presented as Circuit 1 in Fig. 2. The fit to synthetic data obtained from a model for painted steel is presented in Fig. 3. The normalized sum of squares for this fit was found to be 2.055×10^{-14} [*24*]. The measurement model indicates that two time constants can be resolved from the synthetic data, and this result is consistent with the circuit used to generate the synthetic data.

The appearance of a positive imaginary component of the impedance has been attributed at high frequencies to the stray capacity of the current measuring resistor [*31*] and at low frequencies to adsorption phenomena at the electrode surface [*28*]. Transport based models for this behavior are rare, and most electrical circuit models account for this behavior by incorporating either an inductor or a capacitor with a negative value for the capacitance. The measurement model was applied to pseudo-capacitive data reported by Lorenz and Mansfeld [*32*] for corrosion of iron in 0.5 M H_2SO_4. Their model, shown as Circuit 2 in Fig. 2, incorporated an inductor to fit the pseudo-capacitive response at low frequencies. The Voight model can account for inductive behavior if the magnitude (Δ_k) is allowed to have a negative sign. The regression to Circuit 2 is given in Fig. 4. The measurement model indicates that three time constants can be resolved from the synthetic

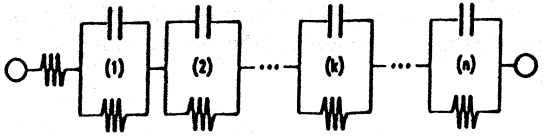

FIG. 1—*The Voight electrical circuit analogue corresponding to the measurement model used in this work (Eq 9).*

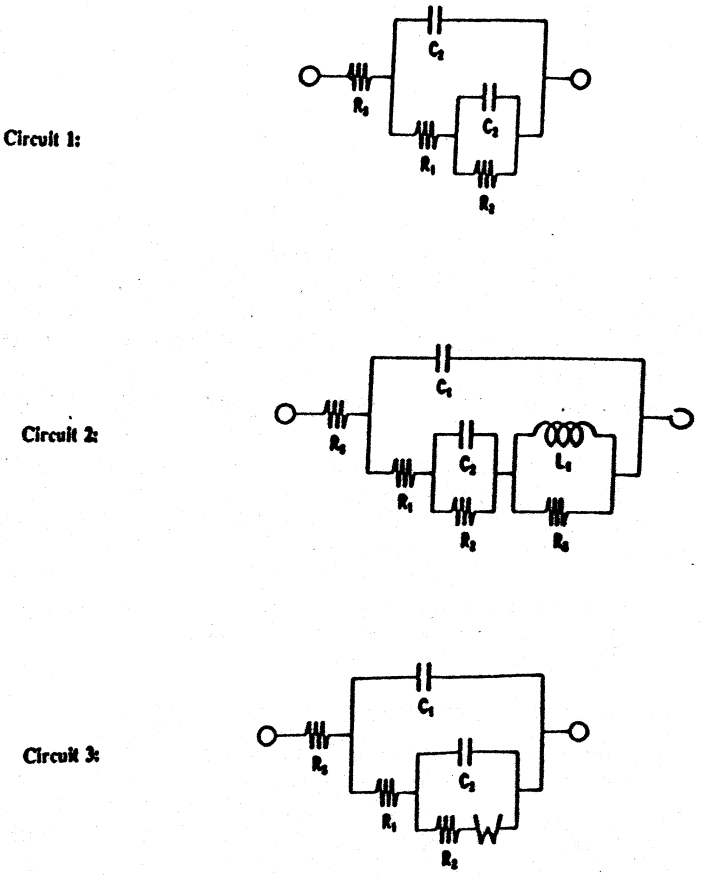

FIG. 2—*Electrical circuit analogues for: (1) corrosion of a painted metal* [30]; *(2) corrosion of iron in 0.5 M* H_2SO_4 *at the corrosion potential* [32]; *and (3) hydrogen evolution on* $LaNi_5$ [15].

data, and this result is fully consistent with the circuit. Complete agreement is obtained because the circuit is composed of only passive elements (one inductor, three resistors, and two capacitors). The residual sum of squares for this fit was found to be 3.221×10^{-14}. The measurement model provides a good fit to data exhibiting an inductive response.

Additional measurement model elements were needed to provide a good fit to systems which contain distributed elements such as are associated with mass transfer limitations and frequency dispersion. In accordance with Eq 9, a measurement model is constructed by sequentially adding k Voight elements with parameters Δ_k and τ_k until the fit is no longer improved by addition of yet another element. This procedure is illustrated for synthetic data obtained from the electrical circuit model proposed for evolution of hydrogen on a $LaNi_5$ ingot electrode [15]. A diffusional resistance was observed in this system as a result of the incorporation of hydrogen into the metal. The electrical circuit model presented as Circuit 3 in Fig. 2 accounted for mass transfer of hydrogen with a Warburg element, and three time constants are evident in the circuit analogue. The complex Warburg impedance, given by

$$Z_w = R_w \frac{\tanh\ (\sqrt{j\tau_w\omega})}{(\sqrt{j\tau_w\omega})} \tag{10}$$

can be derived from the solution of $\nabla^2 c_i = 0$ for a film of thickness δ [28,29]. The time constant can be expressed in terms of diffusivity and film thickness as $\tau_w = \delta^2/D_i$. The Warburg element is sometimes called a distributed element because it can be modeled by a distribution of relaxation times [28]. The optimal regression of the measurement model to synthetic data from Circuit 3 in Fig. 2 required five Voight elements. The fit is presented in Fig. 5, and the resultant residual sum of squares was 4.915×10^{-10}.

The residual sum of squares obtained by fitting the measurement model to the synthetic data is presented as a function of the number of Voight elements in Fig. 6. Figure 6 can be used to show that a maximum of five Voight elements can be resolved from the synthetic data because the sixth Voight element did not improve the quality of the fit. Figure 6 also shows that, while visual inspection of Fig. 5 suggests that a fit obtained with three elements might be acceptable (resulting in residual errors less than 0.1 percent), addition of the fourth and fifth elements provided significant improvement in the residual error. Several points must be made here. The average residual error with five Voight elements was less than 2×10^{-4} percent. The measurement model based on a summation of Voight elements, therefore, provided an excellent fit, despite the fact that the circuit included a Warburg element which has an impedance response that differs significantly from that obtained for a resistor and capacitor in parallel. The measurement model fit the synthetic data to within seven significant figures; therefore, the measurement model can be considered to be statistically adequate to fit the corresponding experimental impedance data for which only three or four significant figures can be expected. To explore the potential influence of experimental error, random noise with a maximum amplitude of five percent was added to the results of Circuit 3. The optimal regression of the measurement model yielded only three Voight circuit elements as shown in Fig. 6. Only three elements could be resolved because the contribution of the fourth circuit element was insignificant as compared to the noise of the data. The normalized sum of squares obtained by regression of the measurement model was slightly lower than the noise level which is shown as a dashed line in Fig. 6.

The comparison of the measurement model to synthetic data, as presented in this section, is meant to illustrate the applicability of the measurement model lineshapes to models that have been developed for "typical" impedance data. The summation of lineshapes associated with the Voight model can be applied to data that can be otherwise modeled by passive elements such as resistors, capacitors, and inductors. It can also be applied to distributed elements such as Warburg and constant phase elements. The model can therefore be used to identify the error structure of impedance data and to evaluate data for consistency with the Kramers-Kronig relations.

Identification of Error Structure

The regression of a measurement model with four Voight elements is presented in Fig. 7 for three replicate impedance spectra obtained for an $In_{0.05}Ga_{0.95}As/GaAs$ superlattice structure on a semi-insulating GaAs substrate [33]. The three data sets are in good agreement, although a larger degree of scatter is evident at low frequencies. The residual error corresponding to Fig. 7 is presented in Fig. 8 as a function of frequency. The scatter evident in the regression can be associated with the frequency-dependent error structure of the data. In this data set, the scatter in the real part of the impedance is largest at high frequencies where the real part of the impedance has become small as compared to the

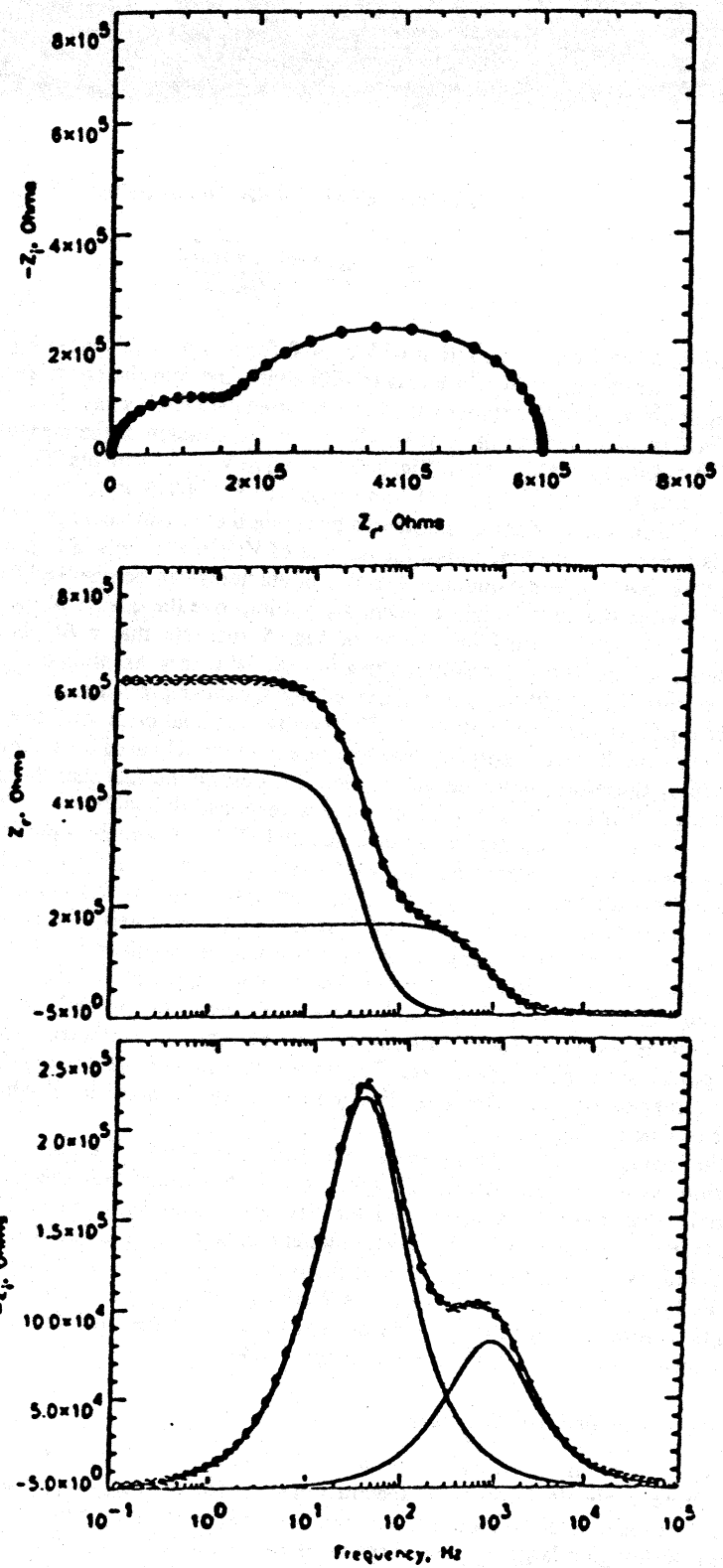

FIG. 3 — *Regression of a measurement model with two Voight elements to synthetic data (○) obtained from Circuit 1 (corrosion of a painted metal [30]). The residual sum of squares for the fit was 2.055 × 10^{-14}. Solid lines in all figures are the results of the model fit. The lines presented in the lower two figures are the model fit and its deconvolution into the contribution of each Voight element. Taken from Ref 24 with permission of the publisher.*

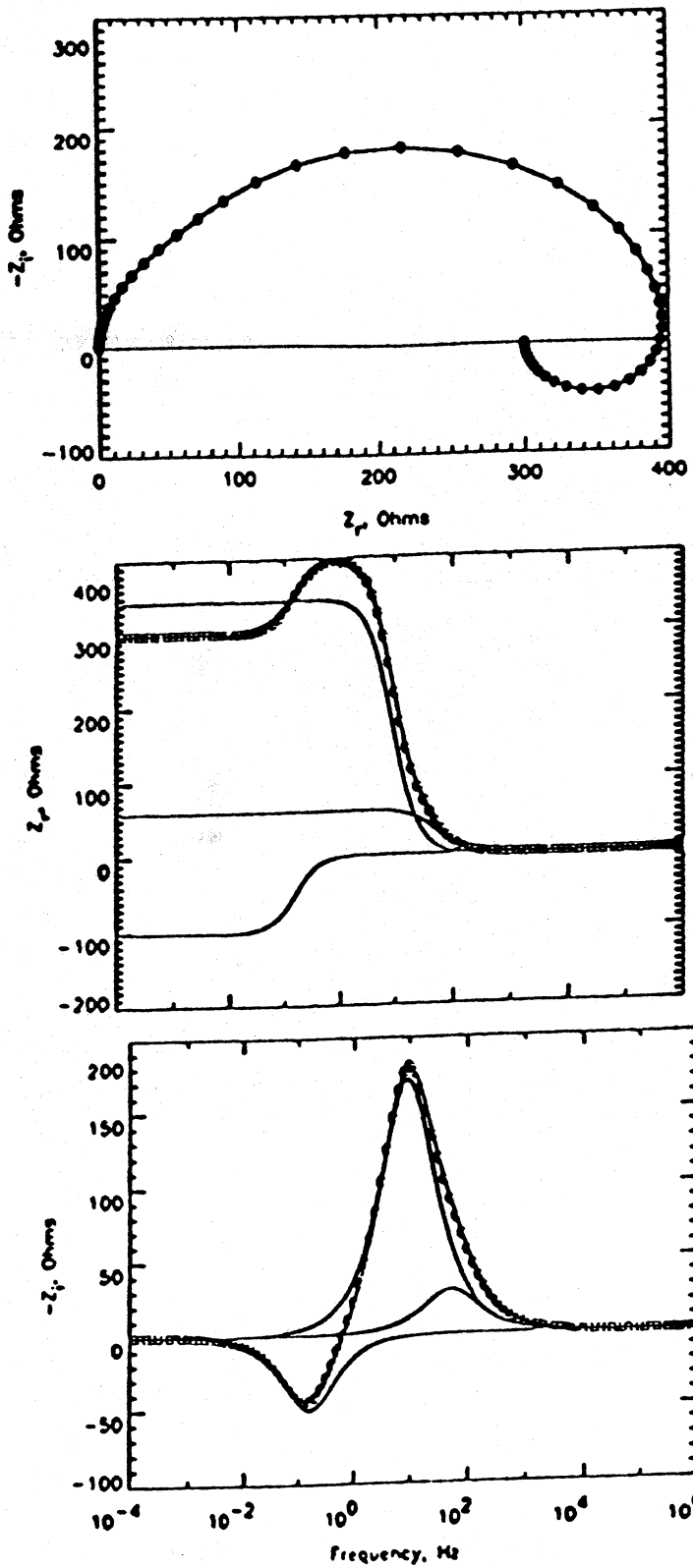

FIG. 4—*Regression of a measurement model with three Voight elements to synthetic data (○) obtained from Circuit 2 (corrosion of iron in 0.5 M H_2SO_4 at the corrosion potential [32]). The residual sum of squares for the fit was 3.221 × 10^{-14}. Solid lines in all figures are the results of the model fit. The lines presented in the lower two figures are the model fit and its deconvolution into the contribution of each Voight element. Taken from Ref 24 with permission of the publisher.*

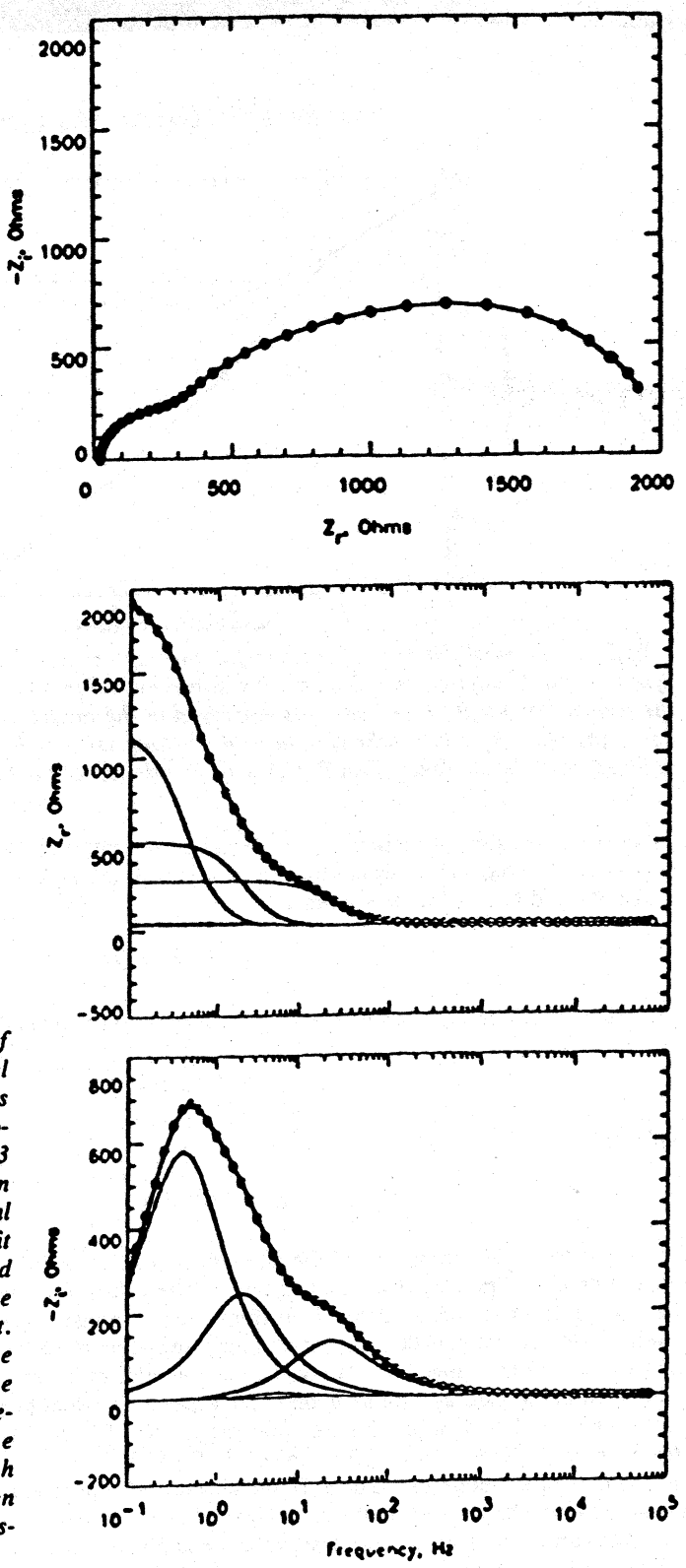

FIG. 5—*Regression of a measurement model with five Voight elements to synthetic data* (○) *obtained from Circuit 3 (hydrogen evolution on* $LaNi_5$ [15]*). The residual sum of squares for the fit was* 4.915×10^{-10}. *Solid lines in all figures are the results of the model fit. The lines presented in the lower two figures are the model fit and its deconvolution into the contribution of each Voight element. Taken from Ref* 24 *with permission of the publisher.*

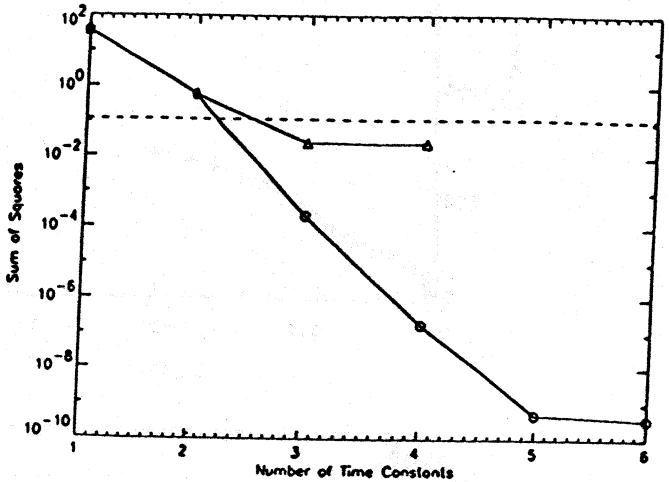

FIG. 6—*Normalized sum of squares for the regression of a measurement model to synthetic data obtained from Circuit 3 (hydrogen evolution on LaNi$_5$ [15]) as a function of the number of Voight time constants employed in the model:* (○) *regression to synthetic data;* (Δ) *regression to synthetic data with random noise added; and (dashed line) normalized noise level. Taken from Ref* 24 *with permission of the publisher.*

value of the imaginary component. Conversely, the scatter in the imaginary component is largest at low frequencies where the real component is dominant.

The dashed line in Fig. 8 is given by

$$\epsilon = \pm 0.01\sqrt{Z_i^2 + Z_r^2}, \tag{11}$$

such that the 95 percent confidence interval for the experimental data is estimated to be

$$Z_r = Z_r^{expt} \pm \epsilon \tag{12}$$

and

$$Z_i = Z_i^{expt} \pm \epsilon \tag{13}$$

The error for each component of the impedance was assumed to be one percent of the magnitude of the impedance at that frequency. The value of one percent was suggested by the specification of the Solartron 1250 frequency response analyzer for variance of the results at 90 percent confidence using a "long integration mode" with a signal greater than 0.02 percent of the range [*34*]. The value used would, of course, be dependent upon the instrumentation used as well as upon other aspects of experimental technique. Work is continuing on identification of more complete models for the frequency-dependent error structure [*35*]. Given its simplicity, however, Eq 11 is in remarkable agreement with the apparent error structure of the data. In the absence of replicate data, Eq 11 could provide an estimate for the variance of the data. Normalization of data by the variance is preferred in regression techniques because least reliance is placed on the least reliable data.

The *a priori* estimate of the error structure of the impedance data can provide a powerful

tool when used in combination with the measurement model. For example, knowledge of the frequency dependence of the expected noise level can be used to interpret the results of "replicate" experiments. The regression of a measurement model with seven Voight elements is presented in Fig. 9 for eight consecutive impedance experiments on $LaNi_5$ at the potential of −0.8 V (Hg/HgO), cathodic to open circuit [*36,37*]. The data presented in Fig. 9 appear replicate, but examination of the residual errors in Fig. 10 reveals that, though the residuals are within twice the standard deviation of the data, the standard deviation of the data is much larger than the expected error structure. The solid lines in Fig. 10 represent twice the standard deviation of the data, and the dashed lines show the estimated error in the data using Eq 11. The errors are not random as would be expected for a truly replicate data set; therefore, the impedance response indicates time-dependent behavior. This analysis shows that the seven runs are not replicate and, instead, reflect the condition of the electrode at different points in time. It is appropriate, therefore, to treat these data as seven independent experimental spectra.

Identification of Consistency with Kramers-Kronig Relations

Most electrochemical impedance data do not adequately approximate the infinite frequency domain required for direct integration of the Kramers-Kronig equations. Experimental spectra can be evaluated for consistency using measurement models without performing integration because measurement models satisfy the Kramers-Kronig relations implicitly. To check for the consistency of the data, the measurement model is regressed to the real or the imaginary part of the experimental spectrum. The model can then be used to predict the other part of the spectrum (i.e., the real part if the regression was done to the imaginary and the imaginary part if the regression was done to the real). From the estimated variance of the model parameters, a 95-percent confidence interval can be found for the model predictions using Monte-Carlo simulation. If the data are within the 95-percent confidence interval, the system can be regarded as being stationary during the course of the experiment. If a significant portion of the data falls outside of the 95-percent confidence interval, the system is likely to be nonstationary. The details of the algorithm for Monte-Carlo simulation are given in Ref *38*. The random number generator used for the simulation was taken from Ref *39*. Five thousand simulations were performed at each frequency to ensure that impedance values follow a Gaussian distribution.

Though the system changed over the period of seven experiments at −0.8 V (Hg/HgO), the measurement model approach demonstrates that a pseudo-steady state approximation applies for each individual run. The applications of the measurement model approach to one experimental data set at −0.8 V (Hg/HgO) is presented in Fig. 11. The measurement model was fit to the imaginary part of the impedance and the confidence interval was predicted for the real part. The circles in Figs. 11 and 12 represent the experimental data, the solid lines represent the 95-percent confidence interval for the model, and the dashed lines in Fig. 12 represent the model for the error structure of the data. The imaginary part of the residuals lie within the proposed error structure, indicating a satisfactory fit of the model to the imaginary part of the data. The use of the error structure to indicate satisfactory regression removes the possibility that a poor fit could be attributed to a local rather than global minimum in the nonlinear regression. Since the real part of the residuals lie within the confidence interval, the data can be deemed to be consistent with the Kramers-Kronig relations. The sharp discontinuity in the residuals at 1000 Hz can be explained by an inappropriate choice of frequency for change of current measuring resistor during the course of the experiment. The measurement model approach can therefore be used to suggest improvements to experimental design.

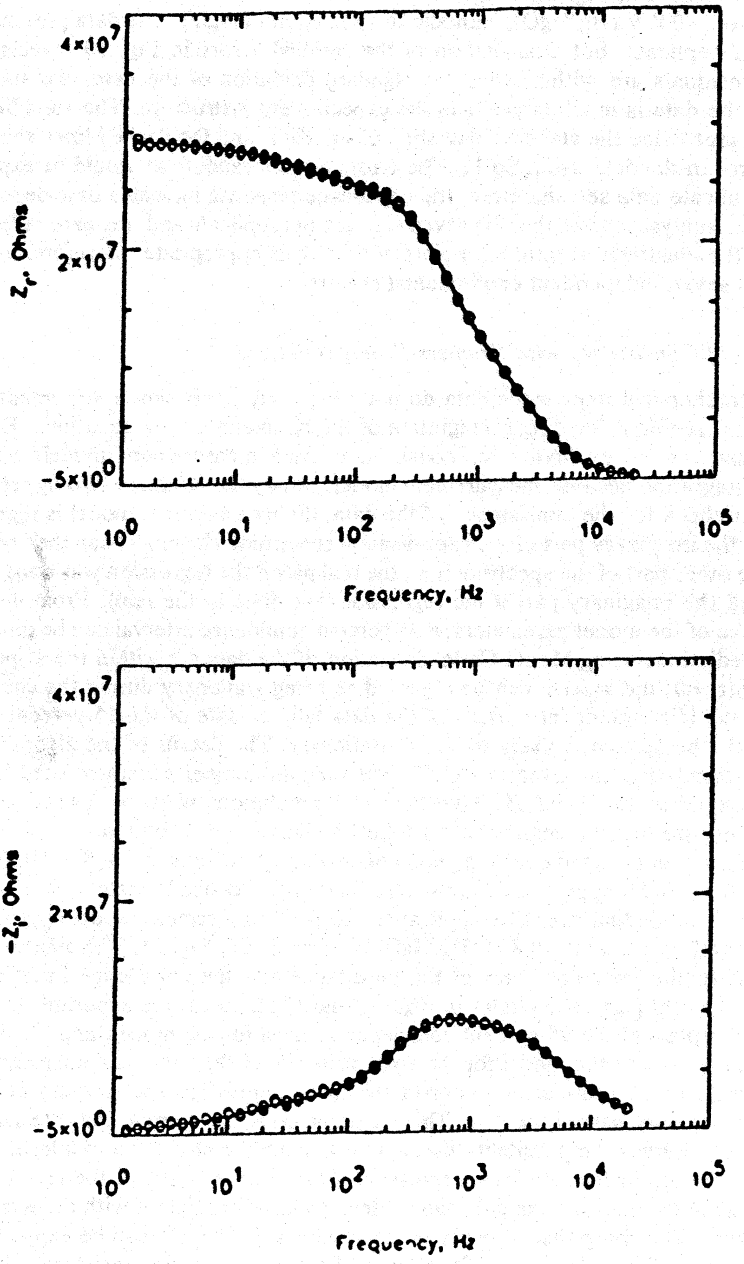

FIG. 7—*Regression of a measurement model with four Voight elements to replicate experimental data* (○) *obtained for an* $In_{0.05}Ga_{0.95}As/GaAs$ *superlattice structure on a semi-insulating GaAs substrate* [33].

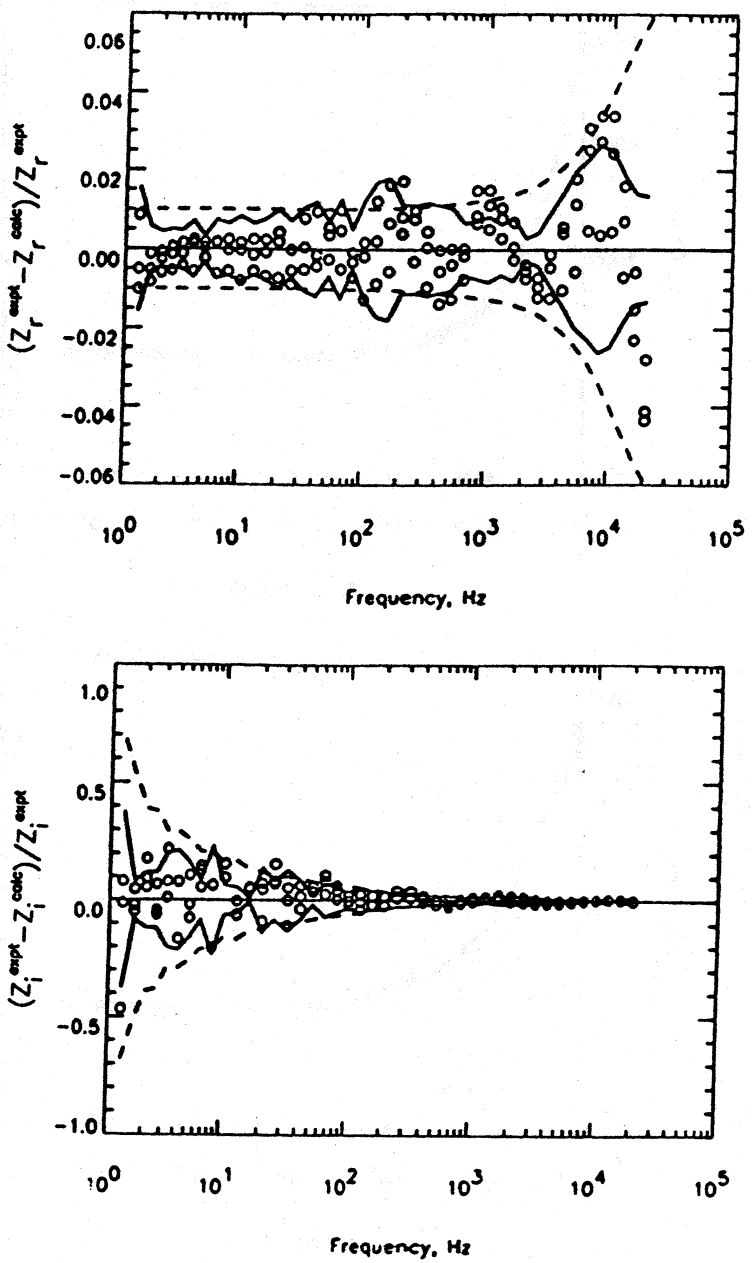

FIG. 8—*Residual error of the regression of a measurement model with four Voight elements to replicate experimental data* (○) *obtained for an* $In_{0.05}Ga_{0.95}As/GaAs$ *superlattice structure on a semi-insulating GaAs substrate. The dashed lines represent a simple model for the error structure of the data given by Eq 11. The solid lines represent the 95-percent confidence interval for the data given at each frequency by twice the standard deviation of the data.*

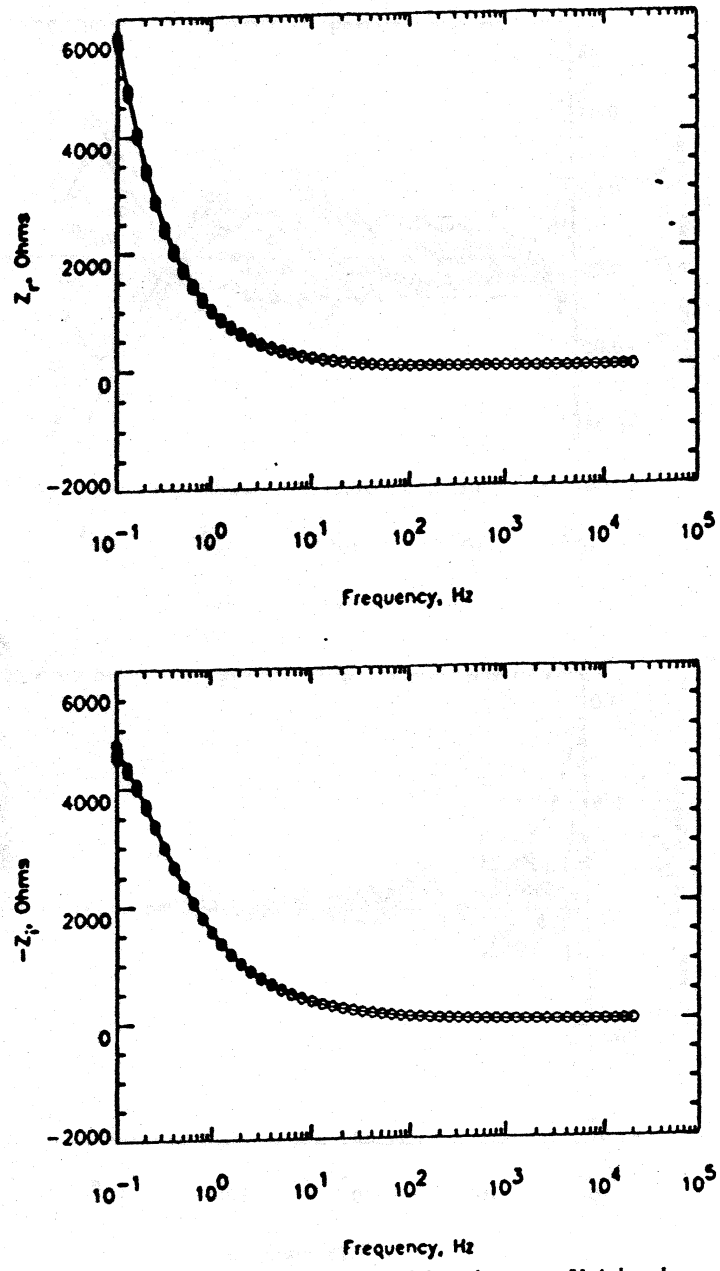

FIG. 9—*Regression of a measurement model with seven Voight elements to eight consecutive impedance scans obtained for a $LaNi_5$ ingot in 31 wt % KOH at a potential of −0.8 V (Hg/HgO)* [35,36]. *The circles represent the experimental data and the lines represent the results of the regression.*

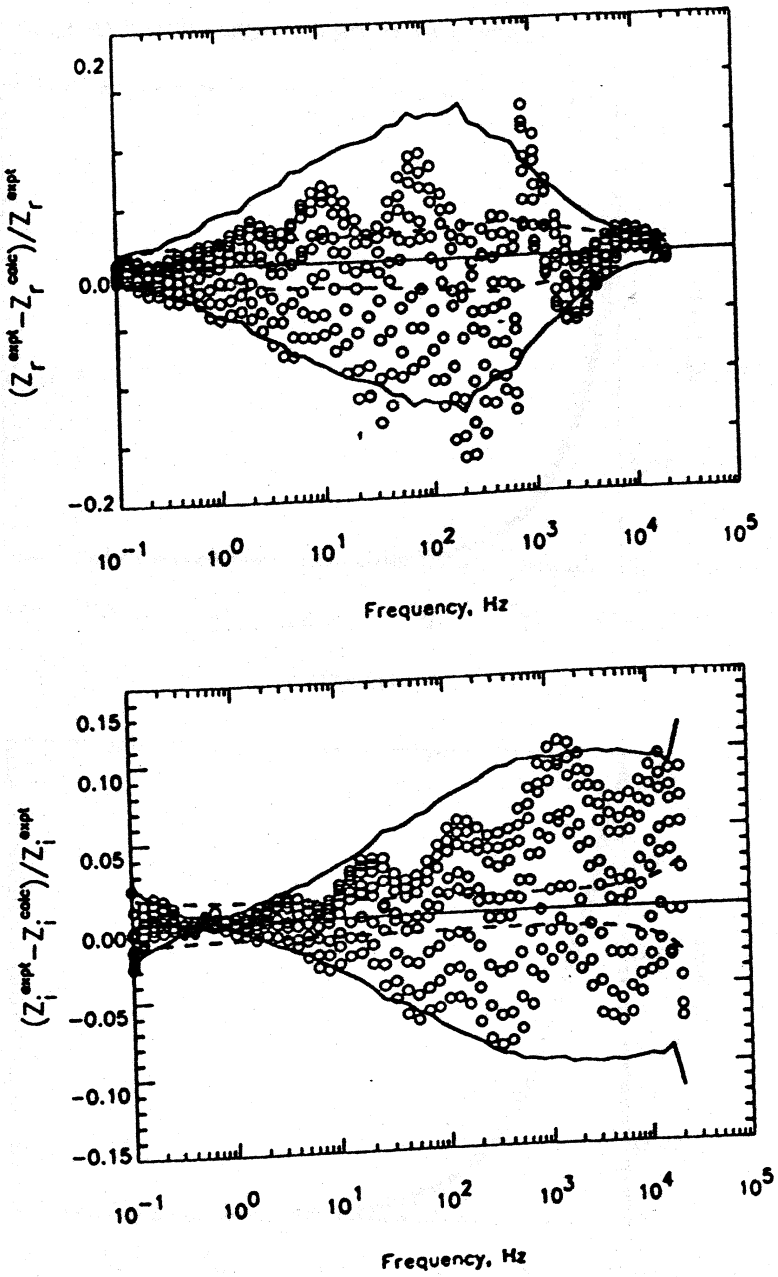

FIG. 10—*Residual errors as a function of frequency for the regression presented in Fig. 9 [35,36]. The circles represent the residual errors, the solid lines represent twice the standard deviation of the data and the dashed lines represent the model for the error structure given by Eq 11.*

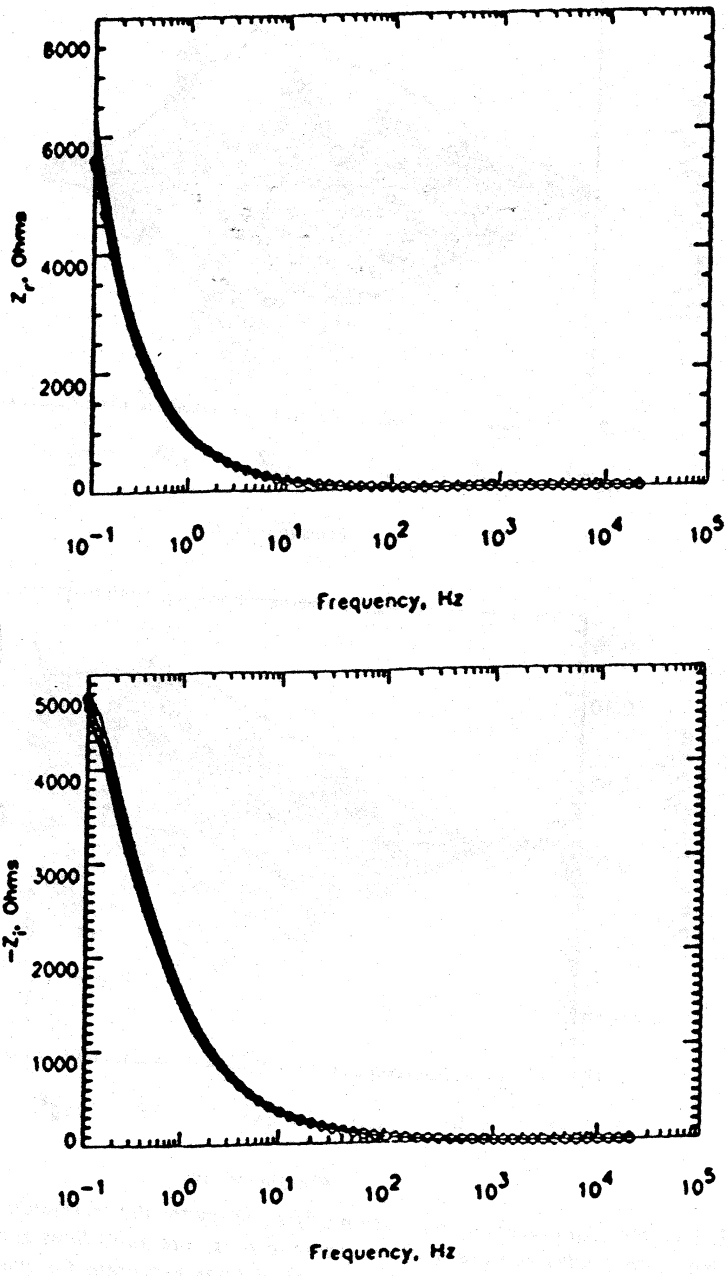

FIG. 11—*Optimal regression of the measurement model to the imaginary part of the impedance spectrum for experimental data obtained for hydrogen evolution at a $LaNi_5$ metal hydride electrode at a potential of −0.8 V (Hg/HgO)* [35,36]. (a) *The real part of the impedance and* (b) *the imaginary part of the impedance. The lines represent the results of the model regression, and the upper and lower lines represent the predicted 95 percent confidence interval for the regression.*

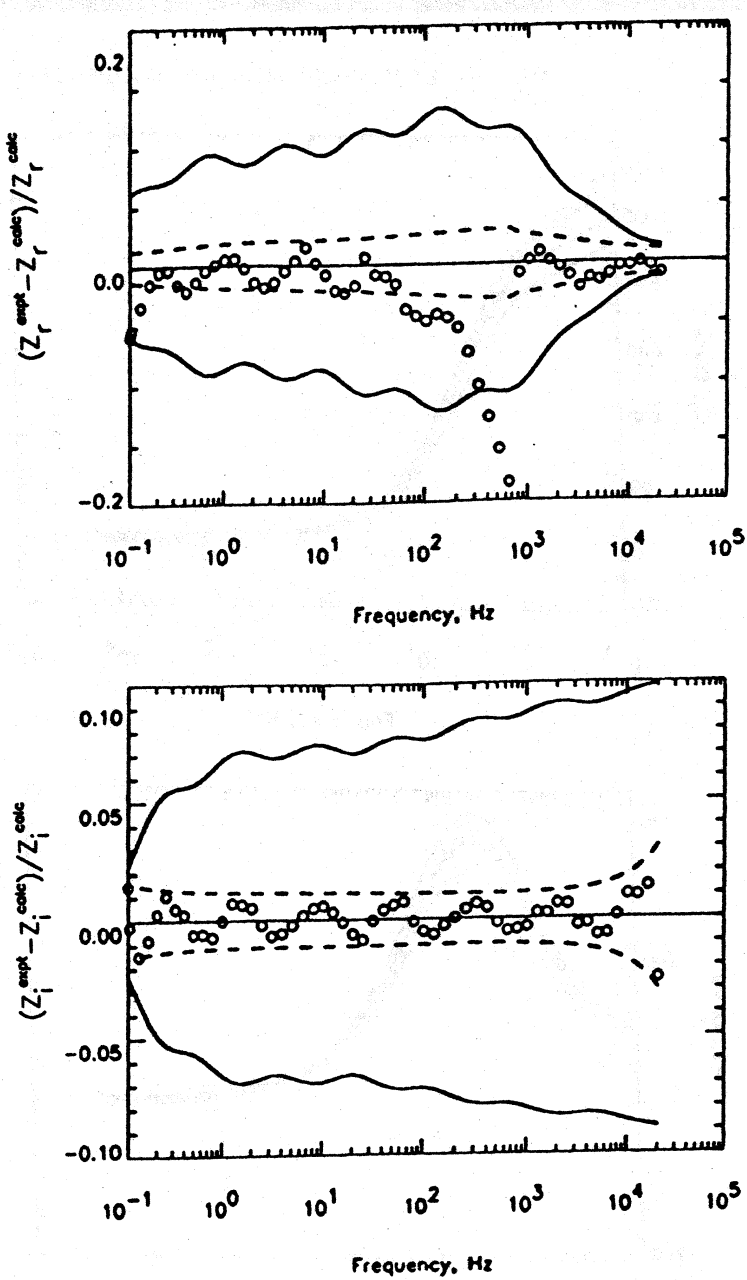

FIG. 12—*Comparison between the residual errors and the predicted 95 percent confidence interval for the model fit to the imaginary part of the impedance spectrum for experimental data obtained for hydrogen evolution at a $LaNi_5$ metal hydride electrode at a potential of −0.8 V (Hg/HgO)* [35,36]. (a) *The real part of the impedance and* (b) *the imaginary part of the impedance. Dashed lines represent the estimated error structure for the data.*

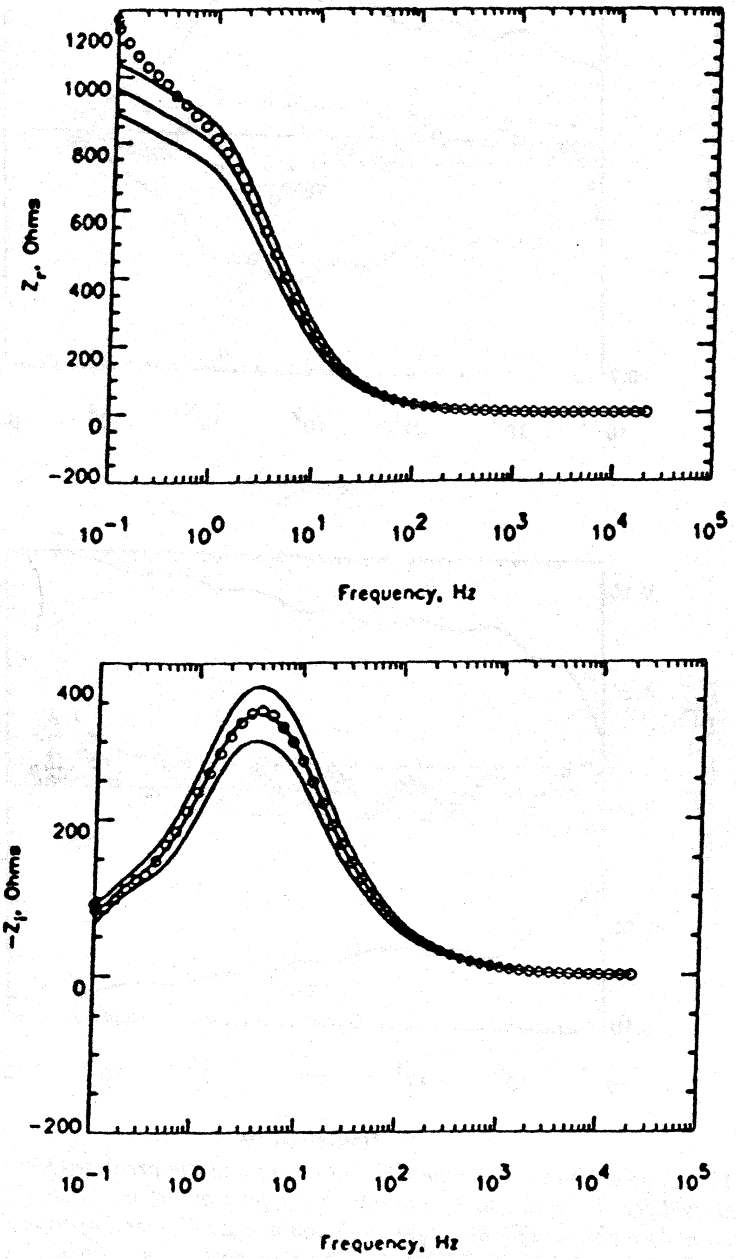

FIG. 13—*Optimal regression of the measurement model to the imaginary part of the impedance spectrum for experimental data obtained for hydrogen evolution at a $LaNi_5$ metal hydride electrode at a potential of −1.1 V (Hg/HgO)* [35,36]. (a) *The real part of the impedance and* (b) *the imaginary part of the impedance. The lines represent the results of the model regression, and the upper and lower lines represent the predicted 95 percent confidence interval for the regression.*

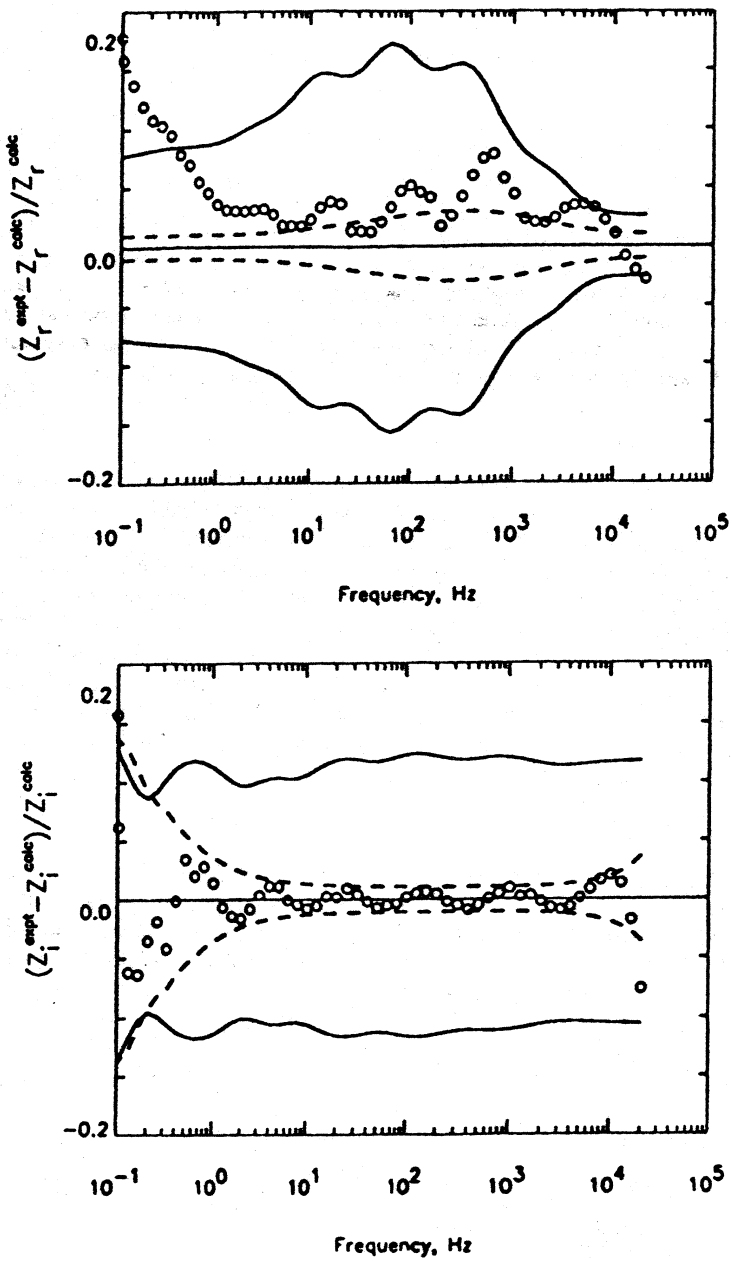

FIG. 14—*Comparison between the residual errors and the predicted 95 percent confidence interval for the model fit to the imaginary part of the impedance spectrum for experimental data obtained for hydrogen evolution at a $LaNi_5$ metal hydride electrode at a potential of −1.1 V (Hg/HgO)* [35,36]. (a) *The real part of the impedance and* (b) *the imaginary part of the impedance. Dashed lines represent the estimated error structure for the data.*

A corresponding analysis is presented in Figs. 13 and 14 for experimental data obtained at −1.1 V (Hg/HgO). The measurement model was regressed to the imaginary part of the impedance and the confidence interval for the real part was predicted. A significant portion of the real part of the spectrum lies outside the 95-percent confidence interval; thus, the data do not satisfy the constraints of the Kramers-Kronig relations. These results are very important for the analysis of the data because most physico-chemical models are developed under the assumption of a pseudo-steady state. These models cannot be used to interpret nonstationary data. The results of the measurement model analysis can be used to suggest changes in the experimental design or to encourage development of models which take the time dependent-behavior of the system into account.

Conclusions

The use of measurement models is superior to the use of polynomial fitting because fewer parameters are needed to model complex behavior and because the measurement model satisfies the Kramers-Kronig relations implicitly. Experimental data can therefore be checked for consistency with the Kramers-Kronig relations without actually integrating the equations over frequency. The use of measurement models does not require extrapolation of the experimental data set; therefore, inaccuracies associated with an incomplete frequency spectrum are resolved. For the application to a preliminary screening of the data, the use of measurement models is superior to the use of more specific electrical circuit analogues because one can determine whether the residual errors are due to an inadequate model, failure of data to conform to the Kramers-Kronig assumptions, or experimental noise.

Acknowledgment

The portion of this work performed at the University of Florida (PAN and MEO) was conducted in support of a series of projects supported by the Office of Naval Research under Grant N00014-89-J-1619 (A. J. Sedriks, Program Monitor), Gates Energy Products, Gainesville, Florida, the National Science Foundation under Grant EET-8617057, and by DARPA under the Optoelectronics program of the Florida Initiative in Advanced Microelectronics and Materials. The work performed at the University of South Florida (LHGR) was supported by the National Science Foundation under Grants RII-8507956 and INT-8602578.

References

[1] Kronig, R. de L., "On the Theory of Dispersion of X-Rays," *Journal of the Optical Society of America and Review of Scientific Instruments*, Vol. 12, 1926, p. 547.

[2] Kronig, R. de L., "Dispersionstheorie im Röntgengebiet," *Physikalische Zeitschrift*, Vol. 30, 1929, p. 521.

[3] Kramers, H. A., "Die Dispersion und Absorption von Röntgenstrahlen," *Physikalische Zeitschrift*, Vol. 30, 1929, p. 522.

[4] Davies, B., "Integral Transforms and Their Applications," in *Applied Mathematical Series 2nd Ed.*, Vol. 25, Springer-Verlag, New York, 1985, p. 101.

[5] Bode, H. W., *Network Analysis and Feedback Amplifier Design*, D. Van Nostrand Company, Inc., NY, 1945.

[6] Gabrielli, C., Keddam, M., and Takenouti, H., "Kramers-Kronig Transformation in Relation to the Interface Regulating Device," *Electrochemical Impedance: Analysis and Interpretation, ASTM STP 1188*, J. R. Scully, D. C. Silverman, and M. W. Kendig, Eds., American Society for Testing and Materials, Philadelphia, 1993 (this publication).

[7] Kendig, M. and Mansfeld, F., "Corrosion Rates From Impedance Measurements: An Improved Approach for Rapid Automatic Analysis," *Corrosion*, Vol. 39, 1983, p. 466.

[8] Macdonald, D. D. and Urquidi-Macdonald, M., "Application of Kramers-Kronig Transforms in the Analysis of Electrochemical Systems: I. Polarization Resistance," *Journal of the Electrochemical Society*, Vol. 132, 1985, p. 2316.

[9] Mansfeld, F., Kendig, M. W., and Lorenz, W. J., "Corrosion Inhibition in Neutral Aerated Media," *Journal of the Electrochemical Society*, Vol. 132, 1985, p. 290.

[10] Urquidi-Macdonald, M., Real, S., and Macdonald, D. D., "Application of Kramers-Kronig Transforms in the Analysis of Electrochemical Systems: II. Transformations in the Complex Plane," *Journal of the Electrochemical Society*, Vol. 133, 1986, p. 2018.

[11] Urquidi-Macdonald, M., Real, S., and Macdonald, D. D., "Applications of Kramers-Kronig Transforms in the Analysis of Electrochemical Impedance Data—III. Stability and Linearity," *Electrochimica Acta*, Vol. 35, 1990, p. 1559.

[12] Dougherty, B. J. and Smedley, S. I., "Validation of Experimental Data from High Impedance Systems Using the Kramers-Kronig Transforms," *Electrochemical Impedance: Analysis and Interpretation, ASTM STP 1188*, J. R. Scully, D. C. Silverman, and M. W. Kendig, Eds., American Society for Testing and Materials, Philadelphia, 1993 (this publication).

[13] Haili, C., "The Corrosion of Iron Rotating Hemispheres in 1M Sulfuric Acid: An Electrochemical Impedance Study," M.S. Thesis, University of California, Berkeley, June 1987.

[14] Esteban, J. M. and Orazem, M. E., "On The Use of the Kramera-Kronig Relations to Evaluate the Consistency of Electrochemical Impedance Data," *Journal of the Electrochemical Society*, Vol. 138, 1991, p. 67.

[15] Orazem, M. E., Esteban, J. M., and Moghissi, O. C., "Practical Applications of the Kramers-Kronig Relations," *Corrosion*, Vol. 47, 1991, p. 248.

[16] Macdonald, D. D. and Urquidi-Macdonald, M., "Kramers-Kronig Transformation of Constant Phase Impedances," *Journal of the Electrochemical Society*, Vol. 137, 1990, p. 515.

[17] Townley, D., "Comments: Evaluation of Kramers-Kronig Transforms for Electrochemical Impedance Data," *Journal of the Electrochemical Society*, Vol. 137, 1990, p. 3305.

[18] Urquidi-Macdonald, M. and Macdonald, D. D., "Comments: Evaluation of Kramers-Kronig Transforms for Electrochemical Impedance Data," *Journal of the Electrochemical Society*, Vol. 137, 1990, p. 3306.

[19] McKubre, M. C. H., Macdonald, D. D., and Macdonald, J. R., "Corrosion of Materials: Kramers-Kronig Transforms," in *Impedance Spectroscopy: Emphasizing Solid Materials and Systems*, J. R. Macdonald, Ed., John Wiley & Sons, New York, 1987, p. 274.

[20] Brachman, M. K. and Macdonald, J. R., "Generalized Immitance Kernels and the Kronig-Kramers Relations," *Physica*, Vol. 20, 1956, pp. 141–148.

[21] Macdonald, J. R. and Potter, Jr., L. D., "A Flexible Procedure for Analyzing Impedance Spectroscopy Results: Description and Illustrations," *Solid State Ionics*, Vol. 23, 1987, pp. 61–79.

[22] Macdonald, J. R., "Impedance Spectroscopy: Old Problems and New Developments," *Electrochimica Acta*, Vol. 35, 1990, pp. 1483–1492.

[23] Macdonald, J. R. and Thompson, W. J., "Strongly Heteroscedastic Nonlinear Regression," *Communication in Statistics—Simulation and Computation*, Vol. 20, 1991, pp. 843–886.

[24] Agarwal, P., Orazem, M. E., and Garcia-Rubio, L. H., "Measurement Models for Electrochemical Impedance Spectroscopy: 1. Demonstration of Applicability," *Journal of the Electrochemical Society*, Vol. 139, 1992, pp. 1917–1927.

[25] Debye, P., *Polar Molecules*, Chemical Catalog Company, New York, 1929.

[26] Christy, R. W., "Classical Theory of Optical Dispersion," *American Journal of Physics*, Vol. 40, 1972, pp. 1403–1419.

[27] Elicabe, G. E., Garcia-Rubio, L. H., and Brandolin, A., "Approximations to the Refractive Index for Light Scattering Measurements," submitted to *Journal of Applied Polymer Science*, 1991.

[28] Raistrick, I. D., Macdonald, J. R., and Franceschetti, D. R., "Theory," Chapter 2 of *Impedance Spectroscopy Emphasizing Solid Materials and Analysis*, J. Ross Macdonald, Ed., John Wiley and Sons, New York, 1987.

[29] Gabrielli, C., *Identification of Electrochemical Processes by Frequency Response Analysis*, Solartron Instrumentation Group Monograph, The Solartron Electronic Group Limited, Farnborough, England, 1980.

[30] Walter, G. W., "A Review of Impedance Plot Methods Used for Corrosion Performance Analysis of Painted Metals," *Corrosion Science*, Vol. 26, 1986, p. 681.

[31] Stewart, K. C., Kolman, D. G., and Taylor, S. R., "The Effect of Parasitic Conduction Pathways on EIS Measurements in Low Conductivity Media," *Electrochemical Impedance:*

Analysis and Interpretation, ASTM STP 1188, J. R. Scully, D. C. Silverman, and M. W. Kendig, Eds., American Society for Testing and Materials, Philadelphia, 1993 (this publication).

[32] Lorenz, W. J. and Mansfeld, F., "Determination of Corrosion Rates by Electrochemical DC and AC Methods," *Corrosion Science*, Vol. 21, 1981, p. 647.

[33] Wojcik, P. T., "Thermally Stimulated Deep-Level Impedance Spectroscopy," M.S. Thesis, University of Florida, August 1992.

[34] *Solartron 1250 Frequency Response Analyzer Operator's Manual*, Schlumberger, Hampshire, England, 1982, p. 17.2.

[35] Agarwal, P., Orazem, M. E., and Garcia-Rubio, L. H., "Measurement Models for Electrochemical Impedance Spectroscopy: 2. The Error-Structure of Impedance Data," in preparation.

[36] Agarwal, P., Orazem, M. E., and Hiser, A., "Application of Electrochemical Impedance Spectroscopy to Metal Hydrides," presented at the 180th Meeting of the Electrochemical Society, Phoenix, AZ, October 13–18, 1991.

[37] Agarwal, P., Orazem, M. E., and Hiser, A., "Application of Electrochemical Impedance Spectroscopy to Metal Hydrides," *Hydrogen Storage Materials, Batteries, and Electrochemistry*, D. A. Corrogan and S. Srinivasan, Eds., The Electrochemical Society, Pennington, NJ, in press.

[38] Agarwal, P., Orazem, M. E., and Garcia-Rubio, L. H., "Measurement Models for Electrochemical Impedance Spectroscopy: 3. Evaluation of Data for Consistency with the Kramers-Kronig Relations," in preparation.

[39] Press, W. H., Flannery, B. P., Teukolsky, S. A., and Vetterling, W. T., *Numerical Recipes, The Art of Scientific Computing*, Cambridge University Press, New York, 1989.